https://doi.org/10.5194/wcd-2020-23
Preprint. Discussion started: 26 May 2020

Weather and Climate Dynamics Discussions
Open Access
EGU

Tropopause-level planetary wave source and its role in two-way troposphere-stratosphere coupling

Lina Boljka[1] and Thomas Birner[2]

[1]Department of Atmospheric Science, Colorado State University, Fort Collins, Colorado, USA
[2]Meteorological Institute, Ludwig-Maximilians-Universität München, Munich, Germany

Correspondence: Lina Boljka (lina.boljka@colostate.edu)

Abstract.

Atmospheric planetary waves play a fundamental role in driving stratospheric dynamics, including sudden stratospheric warming (SSW) events. It is well established that the bulk of the planetary wave activity originates near the surface. However, recent studies have pointed to a planetary wave source near the tropopause that may play an important role in the development of SSWs. Here we analyse the dynamical origin of this wave source and its impact on stratosphere-troposphere coupling, using an idealised model and a quasi-reanalysis. It is shown that the tropopause-level planetary wave source is associated with nonlinear wave-wave interactions and subsequent resonance as well as with transient wave decay. The resulting planetary waves may then propagate deep into the stratosphere, where they dissipate and may help to force SSWs. We find that when an SSW is preceded by the tropopause wave source, it is followed by a robust downward impact, decelerating the tropospheric zonal mean zonal winds between 40-60°N several weeks later. Unlike this robust response following the tropopause wave source events, we do not find such a robust downward impact following the SSWs preceded by surface wave source events. This suggests that the tropopause wave source could potentially be used as one of the predictors of not only SSWs, but their downward impact as well.

1 Introduction

Planetary waves of the extratropical atmosphere are the largest Rossby waves spanning the size of the Earth's radius and longer, and are generally slowly varying (e.g., Burger, 1958; Phillips, 1963). It has been well established in the literature that planetary waves in the Northern Hemisphere (NH) have a source predominantly in the lower troposphere (hereafter surface wave source), primarily associated with orography, land-sea contrasts (e.g., Charney and Eliassen, 1949; Smagorinsky, 1953; Held, 1983; Held and Hoskins, 1985) as well as baroclinic instability (e.g., Charney, 1947; Eady, 1949; Hartmann, 1979) and nonlinear wave-wave interactions (e.g., Scinocca and Haynes, 1998; Domeisen and Plumb, 2012). These planetary waves can propagate upwards reaching the stratosphere, although the bulk of planetary wave activity is dissipated in the upper troposphere

https://doi.org/10.5194/wcd-2020-23
Preprint. Discussion started: 26 May 2020

(e.g., Edmon et al., 1980). The remaining planetary wave activity may propagate deeply into the winter stratosphere where they can disturb the polar vortex via wave-mean flow interactions, decelerating the stratospheric westerly winds (e.g., Charney and Drazin, 1961; Matsuno, 1970, 1971; Holton and Mass, 1976; Limpasuvan et al., 2004). Under extreme situations this results in sudden stratospheric deceleration (SSD) events (Birner and Albers, 2017; Cámara et al., 2019) or sudden stratospheric warming (SSW) events (e.g., Schoeberl, 1978; Butler et al., 2015). SSDs are abrupt decelerations of the stratospheric polar vortex, whereas SSWs require a reversal of the stratospheric winds from the westerlies to the easterlies. Here note that only the planetary scale waves can enter the strong westerlies in the stratospheric polar vortex (Charney and Drazin, 1961).

Wave-mean flow interaction is important for the onset of a stratospheric event, however anomalous surface wave forcing prior to the stratospheric event is not a necessary condition for SSDs or SSWs to occur (e.g., Plumb, 1981; Scott and Polvani, 2004, 2006; Albers and Birner, 2014; Hitchcock and Haynes, 2016; Birner and Albers, 2017; Cámara et al., 2017, 2019). That is, climatological tropospheric wave forcing can be sufficient, depending on the stratospheric state prior to the event. Indeed, only about a third of the SSWs are associated with a strong tropospheric precursor (i.e., wave activity fluxes exceeding 2 standard deviations; Birner and Albers, 2017; Lindgren et al., 2018; Cámara et al., 2019; White et al., 2019). This leaves two thirds of the SSWs that might not be directly related to a tropospheric precursor, suggesting their origin depends on the stratospheric dynamics. This is consistent with Scott and Polvani (2004, 2006), who have shown that even in the absence of a varying troposphere and thus time dependent tropospheric forcing the SSWs still occur. One of the suggested mechanisms for the onset of the SSWs is self-tuning resonance in the stratosphere (e.g., Plumb, 1981; Matthewman and Esler, 2011; Esler and Matthewman, 2011; Lindgren and Sheshadri, 2020), however it is still debated in the literature (e.g., Dunn-Sigouin and Shaw, 2020).

The above studies suggest that anomalous surface wave source is not always necessary for exciting a stratospheric event, and Sjoberg and Birner (2014); Birner and Albers (2017); Cámara et al. (2019) have further argued that the dynamics of the lowermost stratosphere (just above the tropopause) and tropopause inversion layer could be important in exciting the stratospheric events. These studies have also pointed towards a potential planetary wave source just above the tropopause (hereafter tropopause wave source) that precedes the stratospheric events. Indeed, Cámara et al. (2019) found a wavenumber one wave source at the tropopause preceding displacement SSD events regardless of a surface wave source in a comprehensive model and a quasi-reanalysis, whereas for split SSD events this was less clear. This is in contrast with any SSDs/SSWs (regardless of splits or displacements) preceded by a surface wave source, which may exhibit a tropopause wave source following the SSD/SSW events (Birner and Albers, 2017; Cámara et al., 2019). Recent studies have also identified a climatological tropopause wave source (Birner et al., 2013; Dwyer and O'Gorman, 2017) on the poleward side of the subtropical jet stream. Birner et al. (2013) have suggested that it is caused by upscale cascade from synoptic to planetary scale waves when there is a poleward flux of enstrophy (a dynamical mechanism). On the other hand, Dwyer and O'Gorman (2017) have suggested that latent heat release related to convective processes (diabatic effects) can cause a wave source at the tropopause even when planetary waves are not present. These results suggest a presence of a tropopause wave source, which could be associated with the stratospheric events, however its dynamics and impacts have not yet been fully explored.

https://doi.org/10.5194/wcd-2020-23
Preprint. Discussion started: 26 May 2020

The stratospheric events described above are important as they can have a downward impact on the troposphere several weeks after the event (e.g., Baldwin and Dunkerton, 2001; Thompson et al., 2002; Hitchcock and Simpson, 2014), which is typically associated with a negative index in the Northern Annular Mode (NAM) or the North Atlantic Oscillation (NAO), continental cold air outbreaks, and an equatorward shift of the extratropical jet stream. Since the tropospheric signal occurs several weeks later, the stratospheric events also provide a source of predictability of the tropospheric weather regimes beyond the typical weather forecast horizon (e.g., Tripathi et al., 2015; Domeisen et al., 2020). Furthermore, anomalous planetary wave sources that precede an SSW/SSD event can further be used as precursors for predicting the strong disruption of the polar vortex and their later downward impact (e.g., White et al., 2019). This suggests that a better understanding of the planetary wave sources and planetary wave propagation is important for a better understanding and prediction of SSD/SSW events as well as their downward impact. Here we focus on the relatively less explored tropopause planetary wave source, its dynamical origins as well as its impacts on the atmospheric dynamics, especially around SSD and SSW events.

The paper is structured as follows. Section 2 provides theoretical hypotheses for the origin of the tropopause wave source, section 3 provides the methodology, section 4 tests the hypotheses from section 2, and section 5 addresses the impact of the tropopause wave source on two-way stratosphere-troposphere interaction, including a comparison with the surface wave source impacts. Conclusions are given in section 6.

2 What are potential mechanisms for a wave source at the tropopause?

The atmospheric wave sources are generally defined using the Eliassen-Palm (EP) flux (Eliassen and Palm, 1961) divergence, which emerges in wave-mean flow interaction theories within the transformed Eulerian mean perspective (e.g., Andrews and McIntyre, 1976; Edmon et al., 1980). To demonstrate the relations between the eddies and the mean flow we use the quasi-geostrophic (QG) theory, which also provides insight into the more general systems. The QG equations for the eddies and the mean flow are then (e.g., Andrews and McIntyre, 1976; Edmon et al., 1980)

$$\frac{\partial \mathcal{A}}{\partial t} + \nabla \cdot \mathbf{F} = \mathcal{D} \tag{1}$$

$$\frac{\partial [u]}{\partial t} - f[v]^* = \nabla \cdot \mathbf{F} + \mathcal{S} \tag{2}$$

where

$$\mathbf{F} = \left(-[u'v'] \cos\phi, \frac{f[v'\theta']}{\partial[\theta]/\partial p} \right), \tag{3}$$

$\nabla = (\partial/a\partial \sin\phi, \partial/\partial p)$, $\mathbf{F}$ is EP flux, $\mathcal{A} \propto [q'^2]$ is wave activity (q is QG potential vorticity (PV), its square is enstrophy), $\mathcal{D}$ and $\mathcal{S}$ are source-sink terms, $\nabla \cdot \mathbf{F} = [v'q']$ is EP flux divergence (in QG theory it is equal to the meridional PV flux), $[v]^*$ is the meridional component of the residual meridional circulation, u is zonal wind, v is meridional wind, θ is potential temperature, f is Coriolis parameter, p is pressure, ϕ is latitude, t is time, prime ($'$) denotes perturbation from zonal mean, and square brackets ([.]) denote a zonal mean.

https://doi.org/10.5194/wcd-2020-23
Preprint. Discussion started: 26 May 2020

Weather and Climate Dynamics Discussions
Open Access
EGU

EP flux divergence is present in the equation for the waves (Eq. (1)) as well as in the zonal mean zonal wind budget (Eq. (2)). The positive EP flux divergence (via Eq. (1)) represents a wave source ($\nabla \cdot \mathbf{F} > 0$, associated with $\partial \mathcal{A}/\partial t < 0$, i.e., waves leave the region), and the negative EP flux divergence represents a wave sink ($\nabla \cdot \mathbf{F} < 0$, associated with $\partial \mathcal{A}/\partial t > 0$, i.e., waves enter the region). At the same time EP flux divergence appears in Eq. (2), which means that EP flux divergence can affect both the zonal mean zonal wind changes (acceleration ($\partial[u]/\partial t > 0$) if $\nabla \cdot \mathbf{F} > 0$ or deceleration ($\partial[u]/\partial t < 0$) if $\nabla \cdot \mathbf{F} < 0$) or residual meridional circulation changes ($f[v]^* > 0$ if $\nabla \cdot \mathbf{F} < 0$ or $f[v]^* < 0$ if $\nabla \cdot \mathbf{F} > 0$). The changes to the mean flow depend on the depth of the $\nabla \cdot \mathbf{F}$ forcing (e.g., Haynes et al., 1991), i.e., for shallow forcing, such as the surface or tropopause wave source, the zonal mean zonal wind response is weak and the response of the residual circulation dominates, whereas the opposite is true for the deep forcing, such as in the mid-stratosphere.

This illustrates the importance of the EP flux divergence as a wave source and sink, further emphasising the understanding of the origin of the wave sources that occur in the atmosphere. As mentioned in section 1, the wave source at the surface has been studied extensively and can be related to the topography, land-sea contrasts, baroclinic instability etc. (e.g., Charney and Eliassen, 1949; Smagorinsky, 1953; Hartmann, 1979; Scinocca and Haynes, 1998), however little is known about the wave source at the tropopause (e.g., Cámara et al., 2019), which could have a potential impact on the two-way stratosphere-troposphere interactions (more in section 5). In terms of the origin of the tropopause wave source, we explore two dynamical mechanisms: (i) wave decay, and (ii) upscale cascade. Note that the wave decay can only result in an apparent wave source (see below).

2.1 Wave decay

Fig. 1 shows a schematic of a reversible wave growth (panel (a)) and decay (panel (b)) at, e.g., tropopause, which can result in an apparent wave source there (e.g., Hoskins, 1983). As the wave grows (panel (a)) its meridional movements bring low PV air polewards ($q' < 0$, $v' > 0$) and high PV air equatorwards ($q' > 0$, $v' < 0$), resulting in an overall negative meridional PV flux (i.e., $[v'q'] < 0$) and a negative EP flux divergence (i.e., EP flux convergence; recall $\nabla \cdot \mathbf{F} = [v'q']$ in QG theory). Conversely, as the wave decays (panel (b)) its meridional movements bring low PV air equatorwards ($q' < 0$, $v' < 0$) and high PV air polewards ($q' > 0$, $v' > 0$), resulting in an overall positive meridional PV flux (i.e., $[v'q'] > 0$) and positive EP flux divergence. If there is no wave breaking or other effects (e.g., no combination with upscale cascade - see below), this process is reversible and thus an integration over time leaves no positive or negative EP flux divergence (i.e., summing panels (a) and (b) leaves $\nabla \cdot \mathbf{F} = [v'q'] = 0$). Therefore, even if there is a significant increase in positive EP flux divergence, it is an apparent wave source as it represents a wave decay instead.

The apparent wave source at the tropopause could also be caused by the waves entering the region, resulting in negative EP flux divergence ($\nabla \cdot \mathbf{F} < 0$), and later exiting the region, resulting in positive EP flux divergence ($\nabla \cdot \mathbf{F} > 0$). This again leads to $\nabla \cdot \mathbf{F} = 0$ when integrating over time. Note, however, that the exact causes of wave growth and decay are not a subject of this study (see, e.g., Hoskins, 1983).

https://doi.org/10.5194/wcd-2020-23
Preprint. Discussion started: 26 May 2020

Weather and Climate Dynamics Discussions
Open Access
EGU

2.2 Upscale cascade via wave-wave interactions

Fig. 2 shows a schematic of upscale cascade (occurring via wave-wave interactions) and potential subsequent resonance in a vertical cross-section. Assume a wave source (positive EP flux divergence) in lower-to-mid troposphere on the poleward side of the jet stream that can generate waves of various zonal wavenumbers (in the schematic waves of zonal wavenumbers 2, 4, 6 are considered, but in reality they are not limited to those wavenumbers) (see panel (a)). The waves can propagate upwards away from the wave source and dissipate (sink) at the tropopause (negative EP flux divergence). However, as these waves break at the tropopause they may interact with each other nonlinearly, which can lead to upscale cascade.

In the schematic the upscale cascade occurs when the $k = 4$ and $k = 6$ waves interact (where k is zonal wavenumber), leading to $k = 2$ wave generation, and with it a wave source in $k = 2$ occurs (positive EP flux divergence at the tropopause; see panel (b)). If the newly generated wave source for $k = 2$ waves is equal to the wave sink in $k = 4$ and $k = 6$ then the only mechanism at play is upscale cascade. However, if there is a pre-existing wave ($k = 2$) at the tropopause (either a wave with a source below the tropopause (e.g., a stationary wave; as shown in the schematic with an upward grey dashed wiggly arrow) or a growing/decaying wave from Fig. 1) it can interact with newly generated (via upscale cascade) $k = 2$ waves leading to resonance (via selective interference in triad interactions; see, e.g., Chapter 8.1.2 in Vallis, 2006) and amplification of the wave source at the tropopause (thus the wave source at the tropopause in panel (b) is stronger than the wave sink in panel (a)). As a wave at the tropopause is generated, it can propagate in any direction (as denoted in the schematic by $k = 2$ wave propagation), including upward, potentially disturbing the polar vortex in the stratosphere. Note that not all energy from small scale waves is lost in this process, thus some smaller scale waves can still be seen exiting the tropopause wave source/sink region (see $k = 6$ wave propagation in panel (b)). This process results in a clear planetary scale wave source at the tropopause. Here note that while the wave source occurs at the tropopause, the synoptic/planetary scale waves responsible for its growth can originate in the troposphere, thus the troposphere (even if the waves are weak) can indirectly affect the stratospheric dynamics.

2.3 Other potential mechanisms

The wave decay and upscale cascade (with potential resonance) are not the only possible mechanisms causing the wave source at the tropopause in the real atmosphere and are also not mutually exclusive. This means that while there can be upscale cascade and wave decay alone (as discussed above), they can also act together or they are accompanied by other processes, such as diabatic processes (e.g., latent heat release as noted in Dwyer and O'Gorman (2017) or cloud radiative effects - see, e.g., Albers et al. (2016), Fig. 14, which shows $k = 1$ (displacements) and $k = 2$ (splits) pattern in outgoing longwave radiation, potentially suggesting a role of cloud-radiative effects in planetary wave forcing); a meridional or vertical migration of waves before an upscale cascade or wave decay occurs (e.g., a wave source occurs polewards from the wave sink, thus resulting in net wave source in the poleward region; Birner et al., 2013); or other currently unknown dynamical processes. Since one of the main interests of this study is the dynamical origin of the tropopause wave source, we use a dry dynamical core model (described in section 3.1), which lacks the diabatic processes (such as latent heat release or cloud radiative effects), allowing us to assess the dynamical causes of the wave source only, and thus the diabatic effects are not discussed further in this study.

https://doi.org/10.5194/wcd-2020-23
Preprint. Discussion started: 26 May 2020

The two mechanisms (wave decay and upscale cascade) for the origin of a tropopause planetary wave source are tested in section 4, whereas section 5 investigates the impact of wave sources on the two-way stratosphere-troposphere interaction.

3 Methods

3.1 Data

The numerical model used for this study is the dry dynamical core version of the Geophysical Fluid Dynamics Laboratory (GFDL) model with a spectral dynamical core. The model configuration follows Held and Suarez (1994) with some modifications. The model is forced through Newtonian relaxation of the temperature field to a prescribed equilibrium profile, with linear frictional and thermal damping. We use a stratospheric perpetual solstice configuration, following Polvani and Kushner (2002)'s weak polar vortex forcing ($\gamma = 2$) with a troposphere-to-stratosphere transition at 200 hPa (as used in Sheshadri et al., 2015) and a zonal wavenumber 2 mountain with 2 km height following Gerber and Polvani (2009). Note that the tropospheric equilibrium temperature profile was not modified (i.e., follows Held and Suarez, 1994); only the stratospheric profile was. The model resolution is T63 (1.875-degree horizontal resolution at the Equator) with 50 varying vertical levels between 1000 hPa and 0 hPa, and is run for 50005 days, of which the first 300 days are taken as a spin-up period. The zonal mean zonal wind climatology is shown in, e.g., Fig. 8a (black contours) below. The data are analysed as zonal mean and daily mean (from four-times-daily resolution - the eddy fluxes are first computed at 6-hourly resolution and then averaged over 24 h).

As one of the main interests of this study involves the dynamically driven transient behaviour at the tropopause (forced via, e.g., upscale cascade or wave decay mechanisms from section 2), the model configuration differs from the conventionally used strong polar vortex ($\gamma = 4$) with a tall mountain (i.e., 4 km) configuration (e.g., Sheshadri et al., 2015) for the following reasons. If the orographic forcing has a too strong amplitude, there appears to be a direct impact from stationary waves at the tropopause (e.g., see Figs. 5c and 6a in Gerber, 2012), providing a stationary wave source near the tropopause, which leads to a relatively strong climatological positive EP flux divergence there. The goal here is to minimise such a direct impact near the tropopause. Therefore, we have weakened the surface planetary wave forcing, such that its forcing region is limited to 2 km height, which then required a weakening of the polar vortex to obtain a more realistic stratospheric variability and SSD/SSW events with potential downward impact. This yields a weak climatological EP flux divergence at the tropopause (similar in magnitude to the observed values but opposite in sign; not shown), however the model still exhibits strong planetary (mostly $k = 2$) wave variability.

The model results are compared to the ERA-20C quasi-reanalysis (Poli et al., 2016; Martineau et al., 2018), which is provided by the European Centre for Medium-Range Weather Forecasts (ECMWF). The analysis period is 1 January 1900 to 31 December 2010 and data are analysed only for November to March period (i.e. boreal cold season) of every year. The data are analysed on a 1.25° horizontal grid between 1000 hPa and 1 hPa (37 vertical levels). Daily anomalies were computed by subtracting a long-term trend in seasonal cycle (following Cámara et al., 2019). While ERA-20C is not a proper reanalysis dataset (constrained by surface observations only), it provides reasonable stratospheric variability as well as good statistics, which is especially important for studying stratosphere-troposphere interactions (e.g., Gerber and Martineau, 2018; Hitchcock,

https://doi.org/10.5194/wcd-2020-23
Preprint. Discussion started: 26 May 2020

Weather and Climate Dynamics Discussions
Open Access
EGU

2019; Cámara et al., 2019). The underlying model of the ERA-20C also has a very good vertical resolution (91 vertical levels) both in the troposphere and in the stratosphere. Note that we have performed the analysis below also on JRA-55 reanalysis dataset (Kobayashi et al., 2015; Martineau et al., 2018), which yielded qualitatively similar results to ERA-20C, but the statistics were poor (due to small sample sizes), and are thus omitted (for brevity).

3.2 Indices

SSDs are computed following Birner and Albers (2017); Cámara et al. (2019), by finding the largest 10-day drop of the 10 hPa zonal mean zonal wind ($[u]$) averaged between 45 and 75°N (i.e., $\Delta[u]/10$days), after exceeding the 2-standard deviations (2σ) threshold (in ERA-20C that is 20 m/s in 10 days, whereas in the model it is 13 m/s in 10 days). The index is then defined as the mid-point of the deceleration, and the events are required to be separated by at least 20-days. Fig. 3a shows a composite of the standardised stratospheric zonal mean zonal wind anomaly at 10 hPa averaged between 45 and 75°N in the model and in ERA-20C with the centre date during the largest deceleration (i.e., lag 0 is the SSD index), and averaged over all SSD events in each dataset. The evolution is overall similar, with the model deceleration events weaker on average than the ones in ERA-20C, however strengthening of the wind in ERA-20C prior to SSD events (i.e., vortex preconditioning) is absent in the model (see section 5.2.1 for further discussion).

SSWs are defined as a subset of the identified SSDs as the first occurrence of the easterly zonal mean zonal wind (at 10 hPa averaged between 45 and 75°N; cf. Butler et al., 2015) around the SSD event (examining between 5 days prior to the SSD and 20 days after).

The wave source events are defined using the Eliassen-Palm (EP) flux divergence (defined in section 2). Since one of the interests of this paper is the impact of the wave sources on the SSDs and SSWs in the stratosphere where only planetary waves are important, we compute the EP flux divergence that results from planetary scale waves (using Fourier transform). As we are interested in the impact on SSDs/SSWs and not in the distinction of split versus displacement SSW event, we focus on the dominant dynamics in each dataset. The dominant dynamics that is relevant in the stratosphere in ERA-20C is related to $k = 1$ planetary scale waves (e.g., Cámara et al., 2019), however when dry dynamical core models are forced with $k = 1$ forcing (via topography), they do not exhibit SSWs (see, e.g., Table 1 in Sheshadri et al., 2015), thus the model is forced via $k = 2$ planetary waves, which then also represent the dominant stratospheric dynamics in the model. For these reasons, we then compute EP flux divergence for $k = 2$ waves in the model, whereas in ERA-20C we compute EP flux divergence for $k = 1$ waves.

To compute an index at the tropopause we first smooth the data with a 10-day running mean and then find the maximum positive 10-day mean EP flux divergence anomaly that exceeds 0.75σ threshold, and separate events by 20 days. Using stronger thresholds (e.g., 2σ; as used in Birner and Albers, 2017) does not qualitatively change our final results (as it is the duration of the wave forcing that matters; Sjoberg and Birner, 2012), but does result in small sample sizes. The lower-stratospheric level close to the tropopause (in the following thus simply referred to as tropopause level), at which the index is computed, is chosen as the level at which EP flux divergence becomes positive and anomalously strong (exceeding the above threshold) and where it precedes the most SSDs: in the model that is at ∼200 hPa and in ERA-20C it is at ∼225 hPa. The latitudinal average of the wave source is over the latitudinal extent of the wave source region on the poleward side of the extratropical jet-stream

https://doi.org/10.5194/wcd-2020-23
Preprint. Discussion started: 26 May 2020

(40-60°N in the model, and 45-75°N in the reanalyses). Recall that in the model all data are analysed, whereas in ERA-20C only the cold-season wave source events are identified.

As previous studies have used lower-tropospheric wave sources as precursors to SSDs, we use the same methodology as above for the lower tropospheric (surface) wave source, just that now we find the lower-tropospheric level at which EP flux divergence precedes the most SSDs: in the model that is at ∼685 hPa and in reanalyses it is at ∼700 hPa. Note that using vertical EP flux (from Eq. (3)) instead of EP flux divergence yields qualitatively similar results (in the sense that, e.g., zonal mean zonal wind response is similar on average), however vertical EP flux is only a proxy for an actual wave source used here. Note also that using two different indices for the wave sources (i.e., at the tropopause and at the surface) allows us a comparison to previous studies as well as an analysis of the different atmospheric behaviour around, e.g., stratospheric events preceded by the tropopause and by the surface wave source events.

Fig. 3b,c show composites of the standardised EP flux divergence anomaly around wave source events (i.e., lag 0 is the wave source index) at ∼200 hPa and ∼700 hPa, respectively, for the model and ERA-20C. This shows that in both datasets there are long-lived (exceeding the 0.75-σ threshold for over 10 days) wave source events at the tropopause and in the lower troposphere (at surface), and that they have a similar evolution and standardised strength (peaking at 2σ) when they occur.

The wave source indices described here are then used to test if SSDs are preceded by these wave sources, i.e., if SSD occurs within 12 days after wave source event then the SSD is preceded by the wave source event otherwise not. The 12-day horizon is similar to the 10-day horizon used in previous work (e.g., Birner and Albers, 2017; Cámara et al., 2019), which has been identified as a reasonable timescale for wave sources preceding an SSD. Here we again use 12-days to slightly increase the sample size, which does not qualitatively change the results. Some wave source events occur at the same time (i.e., surface wave source occurs when tropopause wave source occurs, generally preceding it), which we have included in the analysis in section 4 (the origin of the tropopause wave source is largely unaffected by this distinction), but we have excluded it from the analysis of SSDs and SSWs in section 5.2 (they generally show a combination of impacts from both wave sources, obscuring their differences), leaving the results for the SSDs preceeded by the tropopause wave source only (i.e., not preceded by the surface wave source), and the SSDs preceded by the surface wave source only (i.e., no tropopause wave source following it before the SSD occurs).

The event statistics are provided in Table 1. We also show the number of events that have been used for each composite in panel-titles in figures below. We used a two-tailed t-test to perform a significance test, where non-significant (two-tailed p-value exceeds 0.05) values are shaded (colours) or excluded (arrows and contours). The data in figures are standardised (as in Fig. 3), i.e., normalised by standard deviation (σ).

3.3 Subjective analysis

In section 4 we test the hypotheses posed in section 2. While we can identify the wave source events and SSDs objectively (section 3.2), and the general picture that emerges follows the ideas presented in section 2, we subjectively identified a handful of cases in the model and in ERA-20C that clearly show the two mechanisms (upscale cascade and wave decay) around SSD

https://doi.org/10.5194/wcd-2020-23
Preprint. Discussion started: 26 May 2020

Weather and Climate Dynamics Discussions
Open Access
EGU

events. This is done as a way of showing that these mechanisms exist, since they can be obscured in an overall average or a randomly chosen case (more often than not they occur simultaneously).

To identify upscale cascade only cases in the model, we compute $k = 2$ EP flux divergence and synoptic ($k \geq 4$) EP flux divergence at the level of the tropopause wave source. We then check the standardised anomalies of both EP flux divergences prior to an SSD event. If there is a negative synoptic EP flux divergence anomaly that is similar in amplitude (exceeding 0.75σ threshold) to the positive $k = 2$ EP flux divergence anomaly before (or at the same time as) the $k = 2$ EP flux divergence peaks, then it is classified as an upscale cascade. At the same time there must not be any strong negative $k = 2$ EP flux divergence preceding the positive $k = 2$ EP flux divergence peak. If there is no negative synoptic EP flux divergence or it is weak, this is not classified as upscale cascade. Note that in ERA-20C we test $k = 2, 3$ EP flux divergence instead of synoptic EP flux divergence, and we test $k = 1$ EP flux divergence instead of $k = 2$ EP flux divergence, since those are the leading contributions to upscale cascade there.

To identify the wave decay mechanism we perform similar analysis as for the upscale cascade mechanism, except that here the synoptic ($k = 2, 3$ in ERA-20C) EP flux divergence anomaly must not be strongly negative prior to the positive peak in $k = 2$ ($k = 1$ in ERA-20C) EP flux divergence anomaly. At the same time there must be a strong negative $k = 2$ ($k = 1$ in ERA-20C) EP flux divergence anomaly preceding the positive $k = 2$ ($k = 1$ in ERA-20C) EP flux divergence anomaly, which are similar in amplitude. This is then identified as the wave decay mechanism rather than the upscale cascade.

4 Evidence for the origin of the tropopause wave source

Section 2 suggested two possible mechanisms for the formation of the wave source at the tropopause: (i) wave decay (resulting in an apparent wave source), and (ii) upscale cascade. Here we test the two hypotheses using subjective analysis (section 3.3) in the model and in ERA-20C. Note that an average over all cases (objectively analysed as per section 3.2) shows indication of both mechanisms as well (see below), thus subjective analysis merely serves to highlight the mechanisms for clear cases of (i) and (ii).

Fig. 4 shows the model's $k = 2$ wave source/sink (anomalous positive/negative EP flux divergence; shading) and anomalous wave propagation (EP fluxes; arrows) in the top panels and synoptic ($k \geq 4$) wave source/sink in the bottom panels for lag-pressure composites over (a,b) all tropopause wave source events preceding SSDs (objective analysis), (c,d) subjectively selected events that demonstrate upscale cascade mechanism, and (e,f) subjectively selected events that demonstrate wave decay mechanism.

Fig. 4c demonstrates a wave source ($k = 2$) at $\sim$200 hPa around lag 0, i.e., the tropopause wave source. This wave source is not preceded by equally strong wave sink at the same level, excluding the possibility of strong wave decay mechanism (consistent with the definitions for subjective analysis; section 3.3). Moreover, Fig. 4d demonstrates a wave sink in the synoptic waves ($k \geq 4$) in the same region and at the same time as the wave source in Fig. 4c, suggesting an upscale cascade mechanism in generating the $k = 2$ wave source (consistent with the hypothesis discussed in section 2.2; see also schematic in Fig. 2). Note that the wave source ($k = 2$) is stronger than wave sink ($k \geq 4$), further suggesting a presence of other mechanisms such

https://doi.org/10.5194/wcd-2020-23
Preprint. Discussion started: 26 May 2020

as resonance (as discussed in section 2.2). The EP fluxes (wave propagation) in Fig. 4c also demonstrate an amplification of wave propagation out of the wave source ($k = 2$) in equatorward and upward direction, which can potentially disturb the stratospheric polar vortex (see section 5).

Fig. 4e demonstrates a wave decay mechanism, which results in an apparent wave source. As in Fig. 4c there is positive EP flux divergence (apparent wave source in $k = 2$ waves) at ∼200 hPa and lag 0, from which waves can propagate equatorwards and upwards, but the propagation is only significant on 90% significance level, thus not shown in Fig. 4e (95% significance level). Note that since this mechanism leads to an apparent wave source we do not necessarily expect wave propagation out of this wave source, unless it is upward wave propagation consistent with a wave entering the tropopause region from below (wave sink) and then exiting it upwards (wave source). The apparent wave source ($k = 2$) here is weaker (compared with panel (c)) and preceded by a similar magnitude negative EP flux divergence ($k = 2$) at the same level, suggesting a wave decay mechanism (consistent with the definitions for subjective analysis; section 3.3), whereby the wave growth results in negative EP flux divergence and wave decay results in positive EP flux divergence (consistent with the hypothesis discussed in section 2.1; see also schematic in Fig. 1). Fig. 4f further demonstrates that upscale cascade does not occur in this case as the synoptic EP flux divergence shows a similar evolution to $k = 2$ EP flux divergence and not the opposite as in Fig. 4d, and it also does not pass the significance threshold.

Fig. 4a shows an average over all wave source ($k = 2$) events preceding SSDs and Fig. 4b shows the same but for the synoptic waves ($k \geq 4$). While the signal is weaker in an average over all events (considering different mechanisms involved in generating the wave source; discussed above; see also section 2) there is still an indication of upscale cascade and potential resonance (wave sink in synoptic waves and a much stronger wave source in $k = 2$ waves at ∼200 hPa and 0 lag), and there is a weak indication of wave decay as well, since there is a very weak negative EP flux divergence ($k = 2$) preceding the positive EP flux divergence ($k = 2$) at the tropopause. The signals of upscale cascade (via negative synoptic EP flux divergence) and wave decay (via negative $k = 2$ EP flux divergence preceding the wave source) are also likely obscured due to cancellations between different mechanisms. The $k = 2$ wave source is strong as both mechanisms lead to enhanced positive $k = 2$ EP flux divergence. Here note that the areas of negative ($k = 2$) EP flux divergence preceding the positive ($k = 2$) EP flux divergence in panel (a) as well as the negative synoptic EP flux divergence in panel (b) exhibit larger areas of significance if 90% significance level is used instead of the 95% (not shown).

While the above results show clear cases of upscale cascade and wave decay in the model, there are many more cases where the distinction is not as clear, suggesting that more often than not both mechanisms play a role in generating a wave source at the tropopause.

Fig. 5 shows the same analysis as in Fig. 4 but for the ERA-20C data. In ERA-20C (as in the real atmosphere) the dominant stratospheric dynamics is related to $k = 1$ waves, thus the top row shows the results for $k = 1$ EP flux divergence and EP fluxes, whereas the bottom row shows EP flux divergence for $k = 2, 3$ waves, since these waves are more important in generating a $k = 1$ wave source at the tropopause than the synoptic waves in ERA-20C (objective analysis, similar to panels (a) and (b), for both the $k = 2, 3$ and the synoptic waves was performed to confirm this; not shown). As in Fig. 4c,d (for the model), Fig. 5c,d demonstrates upscale cascade with positive $k = 1$ EP flux divergence at ∼200 hPa and lag 0 and negative $k = 2, 3$ EP flux

https://doi.org/10.5194/wcd-2020-23
Preprint. Discussion started: 26 May 2020

Weather and Climate Dynamics Discussions
Open Access
EGU

divergence in the same region, but slightly before lag 0. Similarly, Fig. 5e,f demonstrates a wave decay mechanism for $k = 1$ waves (negative EP flux divergence precedes positive EP flux divergence, both having similar magnitude at ∼200 hPa) in panel (e), with panel (f) confirming that upscale cascade is not taking place in this case (no clear wave sink in $k = 2, 3$ waves). As in Fig. 4a,b there is also an indication of upscale cascade and weak wave decay signal in an average over all tropopause wave source events preceding SSDs in Fig. 5a,b, however the wave propagation in ERA-20C is poleward instead of equatorward (partly because of different latitudinal averages in the model and ERA-20C; see also section 5.1). Here note that as in Fig. 4, the regions of significance increase if 90% significance level is used (not shown), which is true especially for the panel (b), where there is a more significant negative $k = 2, 3$ EP flux divergence at the tropopause, as well as for the panel (e), where a more significant negative $k = 1$ EP flux divergence precedes the positive one at the the tropopause.

This section has thus shown that while different waves (in terms of their zonal wavenumber) cause upscale cascade and wave decay in the two datasets, both mechanisms are present in both datasets. As these mechanisms cause a wave source at the tropopause and there is upward wave propagation from this wave source (primarily following the upscale cascade mechanism), we now turn to its impact on two-way stratosphere-troposphere interaction (section 5).

5 Impacts of the planetary wave sources

5.1 Wave source events

Figs. 6 (model), 7 (ERA-20C) show lag-pressure composites over various event types for zonal mean zonal wind anomalies (contours), EP flux divergence anomalies (wave sources/sinks; shading) and EP flux anomalies (wave propagation; arrows). Panels (c) and (f) show the analysis for all tropopause wave source events and all surface wave source events, respectively.

Figs. 6c, 7c clearly show a strong wave source (positive EP flux divergence anomaly) at the tropopause (lower stratosphere) with weak surface wave source occurring at the same time or slightly earlier. While there is some weak wave propagation out of the weak surface wave source, it largely decays in the upper troposphere and/or provides $k = 2$ (model) or $k = 1$ (ERA-20C) waves that can amplify, e.g., upscale cascade leading to resonance (see sections 2.2, 4). Wave propagation out of the tropopause wave source is largely upward, amplified and tilted (equatorward in the model; poleward in ERA-20C). The model and ERA-20C show different meridional direction in wave propagation, which is partly due to different meridional extents when averaging [1], and partly due to the wave source location. The latter means that if the wave source location is very close to strong merged subtropical-extratropical tropospheric jet stream (which acts as a wave guide) as in the model, the waves preferably propagate equatorward in the selected latitudes. On the other hand, in ERA-20C the wave source is further poleward, in the proximity of the extratropical eddy-driven jet stream, and at the same time also closer to the stratospheric polar vortex above, thus poleward propagation of waves is more pronounced than in the model. There is also an indication of reduced upward wave propagation or in some cases even weak downward wave propagation (see downward EP flux anomaly)

[1] In the model we sample the equatorward propagating portion of the waves occurring within the 40-60°N latitudinal band; whereas in ERA-20C we largely sample the poleward propagation of the waves occurring in the 45-75°N latitudinal band; if we average data in the model over 45-75°N latitudinal band we recover more poleward wave propagation, though it is not as strong as in ERA-20C (not shown).

https://doi.org/10.5194/wcd-2020-23
Preprint. Discussion started: 26 May 2020

from the tropopause wave source in both datasets (clearer in ERA-20C). The zonal mean zonal wind anomalies differ between the model and ERA-20C in the troposphere and in the stratosphere prior to wave source event (i.e., before lag 0), however after lag 0 both datasets show wind deceleration in the upper stratosphere, suggesting that the tropopause wave source events may impact the stratospheric winds.

Figs. 6f, 7f clearly show a strong wave source at the surface with weak tropopause wave source occurring slightly later (consistent with the weak link between the surface and tropopause wave sources found in Figs. 6c, 7c). The wave propagation from the surface wave source is largely upward only (less meridional tilting) and amplified as it leaves the wave source region, reaching deep into the stratosphere. As in the case of the tropopause wave source events, there are similar differences between the two datasets also for the surface wave source events, and both datasets suggest zonal mean zonal wind deceleration in the stratosphere (stronger than for the tropopause wave source events) following the surface wave source event (i.e., after lag 0), again suggesting that the surface wave source can help decelerating winds in the stratosphere.

As both the tropopause and the surface wave sources have signals in the zonal mean zonal winds in the stratosphere in both datasets, we discuss below (section 5.2) the composites over the SSD and SSW events to further emphasise the impact of these wave sources. Here note that only a small proportion of all wave source events precede SSDs (Table 1): $\sim$10% of the surface wave source events result in an SSD in both datasets, whereas $\sim$10% (in ERA-20C) and $\sim$4% (in the model) of the tropopause wave source events result in an SSD.

5.2 Two-way stratosphere-troposphere coupling

Panels (a,b,d,e) in Figs. 6 (model), 7 (ERA-20C) show composites of EP flux divergence anomalies, EP flux anomalies and zonal mean zonal wind anomalies centred about an SSD event for (a) all SSD events regardless of wave source, (b) SSD events preceded by tropopause wave source, (d) SSD events not preceded by any wave source, and (e) SSD events preceded by surface wave source.

Figs. 6b,e, 7b,e are similar to Figs. 6c,f, 7c,f, in that they show similar location and amplitude of the tropopause and surface wave sources as well as similar but much stronger wave propagation when composited over the SSD events. Since Figs. 6b,e, 7b,e are composited over SSD events, there is much stronger wind deceleration in the stratosphere than in Figs. 6c,f, 7c,f with some suggestion of a downward impact (see below).

5.2.1 Polar vortex preconditioning

Prior to SSD events (i.e., negative lags in Figs. 6a,b,d,e, 7a,b,d,e) we can observe a positive stratospheric zonal mean zonal wind anomaly, especially for SSDs preceded by surface wave source and SSDs not preceded by either wave source (Figs. 6d,e, 7d,e). This is generally referred to as stratospheric polar vortex preconditioning, which has also been used as one of the potential predictors of SSWs (e.g., Jucker and Reichler, 2018).

In ERA-20C there is a positive zonal mean zonal wind anomaly prior to SSDs (in Fig. 7a,b,d,e; see also Fig. 3a) with some notable differences between the tropopause and surface wave source SSD events. Fig. 7b shows a gradual increase in the stratospheric zonal mean zonal wind, which is much weaker and occurring at lower levels (peaking at $\sim$20 hPa) than for the

https://doi.org/10.5194/wcd-2020-23
Preprint. Discussion started: 26 May 2020

SSDs preceded by the surface wave source (Fig. 7e), where the enhancement of the stratospheric winds occurs more abruptly and at higher levels (peaking at ∼5 hPa).

A similar distinction can also be made in the model (Fig. 6b,e), where SSDs preceded by the tropopause wave source (Fig. 6b) lack the positive stratospheric wind anomaly prior to an SSD, whereas for the SSDs preceded by the surface wave source (Fig. 6e) there is a weak increase in the lower-stratospheric winds prior to an SSD. The lower-stratospheric increase in the zonal mean zonal wind (in Fig. 6a,d,e) is also consistent with Fig. 3a, where no such increase was found at 10 hPa, suggesting that in the model the stratospheric preconditioning might be more pronounced in the lower-stratosphere and thus insignificant at higher levels (unlike in ERA-20C). While there are differences between the model and ERA-20C in terms of the strength and position of the positive zonal mean zonal wind anomaly in the stratosphere, they both suggest that SSDs preceded by the tropopause wave source require much weaker stratospheric preconditioning (if any) than the SSDs preceded by the surface wave source. This distinction is likely a consequence of the tropopause wave source being present in the lower stratosphere already, thus additional preconditioning in that case is not necessary within the stratosphere (unlike for the surface wave source). This further suggests that strong polar vortex (strong negative PV gradients) combined with wave forcing (in this case from the surface wave source), could be used together for predicting the SSDs/SSWs (see also Jucker and Reichler, 2018).

The preconditioning of the stratospheric polar vortex is not only important for SSDs preceded by the surface wave source, but also for SSDs that are not preceded by either of the wave sources (i.e., neither surface nor tropopause wave source; Figs. 6d, 7d), suggesting that stratospheric dynamics play an important role in the evolution of SSDs (e.g., self-tuning resonance; Plumb, 1981; Matthewman and Esler, 2011; Esler and Matthewman, 2011). Here note that in ERA-20C only $k = 1$ wave source events were examined, thus SSDs that are not preceded by $k = 1$ wave sources can still be preceded by $k = 2$ wave sources. Indeed, further analysis (not shown) confirmed that SSDs that are not preceded by $k = 1$ wave source events, show a significant positive $k = 2$ EP flux divergence at the tropopause (but not at the surface), suggesting importance of $k = 2$ waves (see also section 5.2.2). As only the $k = 2$ tropopause wave source (which occurs just above the tropopause in the lower stratosphere) is present, the above suggestion still holds, i.e., stratospheric internal dynamics likely matters.

While there is a positive stratospheric zonal mean zonal wind anomaly prior to an SSD, we can also observe positive tropospheric zonal mean zonal wind anomalies prior to SSDs for both wave sources and in both datasets (Figs. 6b,e, 7b,e), consistent with linear theories of stratosphere-troposphere coupling, where tropospheric and stratospheric wind anomalies are equal in sign (when events are not explosive[2]).

5.2.2 Dynamical evolution around SSD events

As mentioned above, the SSD events can be split into different categories based on the precursory wave source events, such as (i) surface wave source, (ii) tropopause wave source, and (iii) no wave source. These wave sources tend to occur around the beginning of zonal mean zonal wind deceleration in the stratosphere and end as deceleration phases out (see negative EP flux divergence in the stratosphere, a qualitative proxy for $\partial[u]/\partial t$), and they last for over 10 days.

[2]SSDs/SSWs are considered explosive events, which are highly nonlinear; however, weaker anomalous behaviour in the troposphere and stratosphere (such as positive wind anomaly prior to an SSW/SSD) can be consistent with linear dynamics.

https://doi.org/10.5194/wcd-2020-23
Preprint. Discussion started: 26 May 2020

Weather and Climate Dynamics Discussions
Open Access
EGU

When there is a tropopause wave source preceding an SSD (Figs. 6b, 7b), we can see wave propagation out of the wave source (at ∼200 hPa), especially in ERA-20C (Fig. 7b), whereas in the model there is weak wave propagation from the weak surface wave source present as well (which largely dissipates in mid-upper troposphere). In the model (and also in ERA-20C, though not significant in Fig. 7b), the presence of tropospheric $k = 2$ ($k = 1$ in ERA-20C) waves can also contribute to resonance, occurring with upscale cascade at the tropopause (sections 2.2, 4), which further amplifies the wave source and subsequent wave propagation. The waves that originate at the tropopause then dissipate in the stratosphere (negative EP flux divergence there), eventually leading to zonal mean zonal wind deceleration.

SSDs preceded by the surface wave source (Figs. 6e, 7e) show propagation of waves out of the surface wave source, which largely dissipate in the upper-troposphere/lower-stratosphere, especially in ERA-20C. While some of these waves likely make it into deep stratosphere (indicated in the model, but less so in ERA-20C), there is wave amplification occurring within the stratosphere as well, suggesting a role of stratospheric internal dynamics. In ERA-20C it is also possible that smaller scale waves occur via downscale cascade during the wave breaking (dissipation) process, thus no robust $k = 1$ waves are present in the lower-mid stratosphere. However, we found no robust smaller-scale waves (e.g., $k = 2, 3$) in that region, suggesting it may be case dependent (now shown). Additionally, after lag 0 (i.e., after central SSD date) a (weaker) tropopause wave source occurs, which shows clear upward and poleward wave propagation in both datasets, and in ERA-20C there is even an indication of anomalous downward propagation (meaning either weaker upward wave propagation or weak downward wave propagation). The presence of the tropopause wave source following SSDs preceded by surface wave source is consistent with recent studies (e.g., Birner and Albers, 2017; Cámara et al., 2019).

SSDs that are not preceded by neither tropopause nor surface wave source (Figs. 6d, 7d; though in ERA-20C these SSD events can be preceded by $k = 2$ wave source as mentioned above) do not indicate any significant $k = 1$ wave propagation from troposphere to stratosphere in ERA-20C, but weak and discontinuous $k = 2$ wave propagation is present in the model (consistent with weak wave sources there). In ERA-20C (as mentioned above) there is a weak but significant $k = 2$ wave source present at the tropopause (but there is no surface wave source) for SSDs not preceded by $k = 1$ wave source (not shown), which may be the cause of the $k = 2$ wave propagation found within the stratosphere, though a direct link to the $k = 2$ tropopause wave source is not clear. This means that these waves could also be generated via internal stratospheric dynamics, such as self-tuning resonance or downscale cascade. The number of SSDs that are not preceded by any wave source is large (especially in the model; see also Table 1), and excluding the SSDs preceded by the tropopause wave source events (located in the lower stratosphere), leaves only a fraction of SSDs with a tropospheric precursor (tropospheric wave source events; see also Table 1). This suggests that anomalous tropospheric wave forcing is not always necessary for producing SSD events, consistent with, e.g., Sjoberg and Birner (2014); Birner and Albers (2017); Cámara et al. (2019).

When averaging over all SSD events regardless of the wave source (Figs. 6a, 7a) we recover a combination of all of the above discussed cases with the model being dominated by SSDs not preceded by any wave source and SSDs preceded by surface wave source, whereas in ERA-20C a combination of SSDs preceded by surface and tropopause wave sources dominates. Here note that a combination of composites over the tropopause and surface wave source events provides a similar picture to the SSDs preceded by both the surface and tropopause wave source events, which have been omitted from Figs. 6, 7 for clarity.

https://doi.org/10.5194/wcd-2020-23
Preprint. Discussion started: 26 May 2020

Weather and Climate Dynamics Discussions
Open Access
EGU

The above results also explain why meridional heat flux at 100 hPa, a proxy for vertical wave propagation (and vertical EP flux), might not be a good measure of the tropospheric wave forcing. This is because the upward wave propagation at 100 hPa could originate in the troposphere (at the surface), at the tropopause (lower-stratosphere), or even represent internal stratospheric dynamics. While 100 hPa heat flux increases the number of stratospheric events preceded by any precursor by about 30% (compared with the tropospheric, i.e., 700 hPa heat flux index only; e.g, White et al., 2019), its origin is unclear and could also lead to non-robust tropospheric response following the SSD/SSW event (see below). Here we have increased the number of SSDs preceded by any wave source event, by defining surface and tropopause wave source events, which has not been explored before. This means that if we consider surface wave source alone, only about a third of the SSDs are preceded by a wave source event, whereas including the tropopause wave source events increases the number of SSDs preceded by any wave source event by ∼30% in ERA-20C and by ∼13% in the model (see also Table 1). Another ∼10% in the number of SSDs preceded by precursory events can be gained by including SSDs preceded by both wave sources, though their impacts are less clear (not shown). Recall that here the threshold for wave sources was lower than in the previous studies, thus more events have been identified.

5.2.3 Downward impact after SSW events

The zonal mean zonal wind anomalies following the SSD events preceded by the tropopause and surface wave source events show strong deceleration in the stratosphere, which is robust across datasets (Figs. 6, 7), however surface impact is less clear. Fig. 6b,e shows an indication of a weak signal in the troposphere around lags 20 to 30 days following an SSD event, however Fig. 7b,e shows no tropospheric signal. Even though there is some surface signal present following SSD events, it is more common to find surface impact following SSW events, i.e., following a reversal of the stratospheric winds from westerlies to easterlies. Therefore, compositing over the SSW events (Fig. 8), where lag 0 is the first day when the stratospheric zonal mean zonal wind reverses (around an SSD event), yields robust results in the zonal mean zonal wind in the troposphere for the SSWs preceded by the tropopause wave source (Fig. 8a,b), however SSWs preceded by the surface wave source show a weaker and less robust signal (Fig. 8c-f).

For the SSWs preceded by the tropopause wave source (Fig. 8a,b) the model and ERA-20C show wind deceleration in the 40-60 degree latitudinal band at lags 15-25 days following an SSW event. Note that this downward impact can persist for over 20 days (lags 10-30 days and more; not shown), but is the most pronounced between lags 15-25 days. In the model this suggests an equatorward shift of the tropospheric jet stream (merged subtropical-extratropical jet stream), however in ERA-20C this may indicate different processes, since the subtropical and extratropical jet stream can be separated and lie in different locations compared with the model. Therefore, in ERA-20C this may indicate: (i) a weaker eddy-driven (extratropical) jet stream; (ii) an equatorward jet shift of the subtropical jet stream with potentially more quasi-barotropic vertical structure of the subtropical jet stream (there is a robust surface signal and weaker upper-tropospheric signal around 20°N), or (iii) a better split between the subtropical and extratropical jet streams.

Following the SSWs preceded by the surface wave source in the model (Fig. 8c) there is a downward impact similar though weaker than Fig. 8a but for lags 10-20 days with weak persistence up to lags 25-35 days (Fig. 8e; not significant on the 95%

https://doi.org/10.5194/wcd-2020-23
Preprint. Discussion started: 26 May 2020

level but is significant on the 90% level). In ERA-20C (Fig. 8d,f) there is an indication of negative zonal mean zonal wind anomaly between 20 and 40°N as well as between 60 and 80°N with a positive zonal mean zonal wind anomaly in between the two latitudinal bands. While such a pattern persists for lags 10-35 days, the downward impact appears significant first in the 20-60°N latitudinal band (Fig. 8d), and later it is significant (at the surface only) in the 60-80°N latitudinal band (Fig. 8f). The downward impact in ERA-20C (Fig. 8d,f) is therefore different or rather opposite to the downward impact in the model (Fig. 8c,e) when SSWs are preceded by the surface wave source, and the anomalies are weaker (and less robust) than for the SSWs preceded by the tropopause wave source (Fig. 8a,b).

The results for the downward impact on zonal mean zonal winds following SSWs thus show that this impact is different between the SSWs preceded by the tropopause wave source events and those preceded by the surface wave source events. The downward impact of SSWs preceded by the tropopause wave source events is significant and more robust, since ERA-20C and the model show similar and significant results, i.e., the tropospheric wind decelerates in the 40-60°N latitudinal band. Even though the downward impact occurs in a similar latitudinal band, the implications for the tropospheric jet stream changes may differ, e.g., equatorward shift of the tropospheric jet stream in the model versus weakening of the tropospheric jet stream in ERA-20C. On the other hand, the downward impact of SSWs preceded by the surface wave source events, is still significant, but weaker, more confined, and is not robust between the model and ERA-20C. In ERA-20C the downward impact is in the 20-40°N and 60-80°N latitudinal bands, whereas in the model it is in the 40-60°N latitudinal band (as for the tropopause wave source). While the model shows similar downward impact for both wave sources, there are notable differences in ERA-20C, which is a better representation of the real atmosphere. This suggests that care must be taken when using indices (as also mentioned above), such as 100 hPa heat flux, since the downward impact (that we would ultimately like to predict) might be different depending on the origin of the waves at 100 hPa level (i.e., wave originating at the tropopause or at the surface).

Note that for SSDs/SSWs that are not preceded by any wave source events, and for averages over all SSD/SSW events, no robust signal was found in the zonal mean zonal winds in the troposphere (not shown).

6 Conclusions

Recent work has identified a planetary wave source just above the tropopause, both in a climatological sense on the poleward side of the subtropical jet stream (Birner et al., 2013), as well as transiently on the poleward side of the extratropical jet stream, preceding the SSD events (Cámara et al., 2019). This study has examined the dynamical origins of the tropopause planetary wave source on the poleward side of the extratropical jet stream and its impacts on two-way stratosphere-troposphere coupling. A better understanding of the tropopause wave source and its impacts may provide additional precursors to stratospheric events (SSDs, SSWs), potentially leading to a better prediction of the strong stratospheric events and their downward impact.

By analysing an idealised, mechanistic general circulation model (dry dynamical core), and ERA-20C quasi-reanalysis, we have shown that the tropopause wave source can occur through upscale cascade and subsequent resonance (Figs. 2, 4c,d, 5c,d) as well as through wave decay (resulting in an apparent wave source; Figs. 1, 4e, 5e) in both datasets. While cases where only upscale cascade with resonance or only wave decay exist, they are more commonly occurring together, further amplifying the

https://doi.org/10.5194/wcd-2020-23
Preprint. Discussion started: 26 May 2020

wave source signal at the tropopause. When the tropopause wave source occurs the planetary waves then propagate out of the wave source region in all directions (upwards, equatorwards, polewards and even downwards; Figs. 6c, 7c), which can affect the atmospheric dynamics in the troposphere as well as stratosphere. As the waves propagate vertically into the stratosphere where they break and dissipate, they can decelerate the westerlies in the polar vortex (as indicated in Figs. 6c, 7c), which can lead to SSD and/or SSW events.

While only a small fraction of all tropopause wave source events (∼4% in the model, ∼10% in ERA-20C; Table 1) lead to SSD/SSW events (Figs. 6b, 7b), they overall help increasing the number of SSDs/SSWs preceded by any wave source event (i.e., in addition to the surface wave source events), thus increasing the number of stratospheric events with a precursory wave source event, which is important for their predictability. Additionally, the SSW events preceded by the tropopause wave source have a robust downward impact in both datasets - there is a deceleration of the tropospheric zonal mean zonal winds in the 40-60°N latitudinal band ∼15-25 days after the SSW event (Fig. 8a,b), further suggesting potential for predictability.

A comparison with the surface wave source events and their impact on the two-way stratosphere-troposphere coupling (Figs. 6e,f, 7e,f) reveals that a (weaker) tropopause wave source occurs following the surface wave source and SSD/SSW events (see also Birner and Albers, 2017; Cámara et al., 2019) as well as that the waves originating in the surface wave source largely sink in the upper troposphere, of which some make it into the stratosphere where they break (dissipate) and decelerate the zonal mean zonal winds. When a tropopause wave source occurs following SSDs preceded by a surface wave source, there is also an indication of upward planetary wave propagation from this wave source, which could also be an indication of a positive feedback between a wave near the tropopause and a wave along the polar vortex. While there is a downward impact following SSWs preceded by the surface wave source event (Fig. 8c-f), it is less robust, with the model having a downward impact ∼10-20 days after the SSW event, which is similar (but weaker) to the SSWs preceded by the tropopause wave source, whereas ERA-20C shows a (weak) downward impact first further equatorward and later on further poleward.

The robust response of the tropospheric zonal mean zonal wind following SSDs/SSWs preceded by the tropopause wave source events (unlike for the surface wave source events), could suggest that the downward coupling following SSDs/SSWs is clearer when the (lower) stratospheric dynamics dominate the onset of the SSDs/SSWs. This means that if the troposphere does not have anomalous planetary waves prior to the SSD/SSW event its response could be stronger. This could be because the planetary and synoptic waves can have opposing effects on driving of the zonal wind (e.g., Hoskins et al., 1983), thus if the tropospheric planetary waves are weak, the response could be dominated by the synoptic waves and thus clearer.

The very different signal in tropospheric zonal mean zonal winds following SSWs preceded by surface versus tropopause wave source events in ERA-20C as well as the presence of two different types of wave source events, also suggest that care must be taken when using indices, such as 100 hPa heat flux (see also Cámara et al., 2017). This is because: (i) the waves occurring at 100 hPa can be excited at the surface or at the tropopause (shown here), or even internally within the stratosphere (e.g., Plumb, 1981); and (ii) the SSWs preceded by the tropopause wave source lead to a clear, robust and significant downward impact (in 40-60°N latitudinal band), whereas SSWs preceded by surface wave source lead to weaker and opposite non-robust surface signal.

https://doi.org/10.5194/wcd-2020-23
Preprint. Discussion started: 26 May 2020

Furthermore, we have also shown that the polar vortex preconditioning, i.e., strengthening of the polar vortex prior to SSD events (which can also be used as one of the precursors to SSDs; e.g., Jucker and Reichler, 2018) could be different between the SSDs preceded by tropopause and surface wave source events. This means that SSDs preceded by the tropopause wave source events are generally related to weaker (if any) zonal mean zonal wind strengthening (i.e., negative PV gradients) prior to SSDs (weak/no polar vortex preconditioning necessary), whereas SSDs preceded by surface wave source events are related to significant strengthening of the zonal mean zonal wind prior to SSDs (i.e., polar vortex preconditioning is necessary).

In summary, this study has addressed the dynamical origin of the tropopause wave source and analysed its impact on the two-way stratosphere-troposphere coupling. While this work has focused on the dynamical origins of the tropopause wave source, other potential wave sources with, e.g., a diabatic (via latent heat release) origin could be explored in the future, by, e.g., employing a hierarchy of models approach (e.g., Hoskins, 1983; Held, 2005). Further work is also necessary to test whether the tropopause wave source could be used as one of the predictors of the SSD/SSW events and their downward impact in, e.g., the subseasonal-to-seasonal model datasets (Vitart et al., 2017; Pegion et al., 2019).

Code availability. The model code is available on GitHub (https://github.com/lukelbd/gfdl-fms). The parameters are specified in section 3.1 and in Polvani and Kushner (2002); Gerber and Polvani (2009). Other scripts are available upon request.

Data availability. ERA-20C data was obtained from the European Centre for Medium Range Forecasts website (https://apps.ecmwf.int/datasets/data/era20c-daily/levtype=pl/type=an/).

Author contributions. LB performed the model experiment and its analysis. TB and LB analysed ERA-20C data. The figures were prepared by LB and TB, and the first draft of the manuscript was prepared by LB, which was further improved by TB for the final version.

Competing interests. The authors declare that they have no conflict of interest.

Acknowledgements. This study was funded by the National Science Foundation Grant number AGS-1643167. We thank Luke Davis for the help with the model and Dave Thompson for helpful discussions.

https://doi.org/10.5194/wcd-2020-23
Preprint. Discussion started: 26 May 2020

Weather and Climate Dynamics Discussions
Open Access
EGU

References

Albers, J. R. and Birner, T.: Vortex Preconditioning due to Planetary and Gravity Waves prior to Sudden Stratospheric Warmings, Journal of the Atmospheric Sciences, 71, 4028–4054, https://doi.org/10.1175/JAS-D-14-0026.1, 2014.

Albers, J. R., Kiladis, G. N., Birner, T., and Dias, J.: Tropical Upper-Tropospheric Potential Vorticity Intrusions during Sudden Stratospheric Warmings, Journal of the Atmospheric Sciences, 73, 2361–2384, https://doi.org/10.1175/JAS-D-15-0238.1, 2016.

Andrews, D. G. and McIntyre, M. E.: Planetary waves in horizontal and vertical shear: the generalized Eliassen-Palm relation and the mean zonal acceleration, J. Atmos. Sci., 33, 2031–2048, 1976.

Baldwin, M. P. and Dunkerton, T. J.: Stratospheric Harbingers of Anomalous Weather Regimes, Science, 294, 581–584, https://doi.org/10.1126/science.1063315, 2001.

Birner, T. and Albers, J. R.: Sudden Stratospheric Warmings and Anomalous Upward Wave Activity Flux, SOLA, 13A, 8–12, https://doi.org/10.2151/sola.13A-002, 2017.

Birner, T., Thompson, D. W. J., and Shepherd, T. G.: Up-gradient eddy fluxes of potential vorticity near the subtropical jet, Geophys. Res. Lett., 40, 5988–5993, https://doi.org/10.1002/2013GL057728, 2013.

Burger, A. P.: Scale Consideration of Planetary Motions of the Atmosphere, Tellus, 10, 195–205, https://doi.org/10.1111/j.2153-3490.1958.tb02005.x, 1958.

Butler, A. H., Seidel, D. J., Hardiman, S. C., Butchart, N., Birner, T., and Match, A.: Defining Sudden Stratospheric Warmings, Bulletin of the American Meteorological Society, 96, 1913–1928, https://doi.org/10.1175/BAMS-D-13-00173.1, 2015.

Cámara, A. d. l., Albers, J. R., Birner, T., Garcia, R. R., Hitchcock, P., Kinnison, D. E., and Smith, A. K.: Sensitivity of Sudden Stratospheric Warmings to Previous Stratospheric Conditions, Journal of the Atmospheric Sciences, 74, 2857–2877, https://doi.org/10.1175/JAS-D-17-0136.1, 2017.

Cámara, A. d. l., Birner, T., and Albers, J. R.: Are Sudden Stratospheric Warmings Preceded by Anomalous Tropospheric Wave Activity?, Journal of Climate, 32, 7173–7189, https://doi.org/10.1175/JCLI-D-19-0269.1, 2019.

Charney, J. G.: THE DYNAMICS OF LONG WAVES IN A BAROCLINIC WESTERLY CURRENT, Journal of Meteorology, 4, 136–162, https://doi.org/10.1175/1520-0469(1947)004<0136:TDOLWI>2.0.CO;2, 1947.

Charney, J. G. and Drazin, P. G.: Propagation of planetary-scale disturbances from the lower into the upper atmosphere, Journal of Geophysical Research (1896-1977), 66, 83–109, https://doi.org/10.1029/JZ066i001p00083, 1961.

Charney, J. G. and Eliassen, A.: A Numerical Method for Predicting the Perturbations of the Middle Latitude Westerlies, Tellus, 1, 38–54, https://doi.org/10.1111/j.2153-3490.1949.tb01258.x, 1949.

Domeisen, D. I. V. and Plumb, R. A.: Traveling planetary-scale Rossby waves in the winter stratosphere: The role of tropospheric baroclinic instability, Geophysical Research Letters, 39, L20 817, https://doi.org/10.1029/2012GL053684, 2012.

Domeisen, D. I. V., Butler, A. H., Charlton-Perez, A. J., Ayarzagüena, B., Baldwin, M. P., Dunn-Sigouin, E., Furtado, J. C., Garfinkel, C. I., Hitchcock, P., Karpechko, A. Y., Kim, H., Knight, J., Lang, A. L., Lim, E.-P., Marshall, A., Roff, G., Schwartz, C., Simpson, I. R., Son, S.-W., and Taguchi, M.: The Role of the Stratosphere in Subseasonal to Seasonal Prediction: 2. Predictability Arising From Stratosphere-Troposphere Coupling, Journal of Geophysical Research: Atmospheres, 125, e2019JD030 923, https://doi.org/10.1029/2019JD030923, 2020.

Dunn-Sigouin, E. and Shaw, T.: Dynamics of anomalous stratospheric eddy heat flux events in an idealized model, Journal of the Atmospheric Sciences, Accepted, https://doi.org/10.1175/JAS-D-19-0231.1, 2020.

https://doi.org/10.5194/wcd-2020-23
Preprint. Discussion started: 26 May 2020

Dwyer, J. G. and O'Gorman, P. A.: Moist Formulations of the Eliassen–Palm Flux and Their Connection to the Surface Westerlies, Journal of the Atmospheric Sciences, 74, 513–530, https://doi.org/10.1175/JAS-D-16-0111.1, 2017.

Eady, E. T.: Long Waves and Cyclone Waves, Tellus, 1, 33–52, https://doi.org/10.1111/j.2153-3490.1949.tb01265.x, 1949.

Edmon, H. J., Hoskins, B. J., and McIntyre, M. E.: Eliassen-Palm cross sections for the troposphere, J. Atmos. Sci., 37, 2600–2616, 1980.

Eliassen, A. and Palm, E.: On the transfer of energy in stationary mountain waves, Geofys. Pub., 22, 1–3, 1961.

Esler, J. G. and Matthewman, N. J.: Stratospheric Sudden Warmings as Self-Tuning Resonances. Part II: Vortex Displacement Events, Journal of the Atmospheric Sciences, 68, 2505–2523, https://doi.org/10.1175/JAS-D-11-08.1, 2011.

Gerber, E. P.: Stratospheric versus Tropospheric Control of the Strength and Structure of the Brewer–Dobson Circulation, Journal of the Atmospheric Sciences, 69, 2857–2877, https://doi.org/10.1175/JAS-D-11-0341.1, 2012.

Gerber, E. P. and Martineau, P.: Quantifying the variability of the annular modes: reanalysis uncertainty vs. sampling uncertainty, Atmospheric Chemistry and Physics, 18, 17 099–17 117, https://doi.org/10.5194/acp-18-17099-2018, 2018.

Gerber, E. P. and Polvani, L. M.: Stratosphere–Troposphere Coupling in a Relatively Simple AGCM: The Importance of Stratospheric Variability, Journal of Climate, 22, 1920–1933, https://doi.org/10.1175/2008JCLI2548.1, 2009.

Hartmann, D. L.: Baroclinic Instability of Realistic Zonal-Mean States to Planetary Waves1, Journal of the Atmospheric Sciences, 36, 2336–2349, https://doi.org/10.1175/1520-0469(1979)036<2336:BIORZM>2.0.CO;2, 1979.

Haynes, P. H., McIntyre, M. E., Shepherd, T. G., Marks, C. J., and Shine, K. P.: On the "Downward Control" of Extratropical Diabatic Circulations by Eddy-Induced Mean Zonal Forces, Journal of the Atmospheric Sciences, 48, 651–678, https://doi.org/10.1175/1520-0469(1991)048<0651:OTCOED>2.0.CO;2, 1991.

Held, I. M.: Stationary and quasi-stationary eddies in the extratropical troposphere: theory. In Large-Scale Dynamical Processes in the Atmosphere (B. J. Hoskins and R. Pearce, eds.), Academic Press, 1983.

Held, I. M.: The gap between simulation and understanding in climate modeling, Bull. Am. Meteorol. Soc., 86, 1609 – 1614, 2005.

Held, I. M. and Hoskins, B. J.: Large-Scale Eddies and the General Circulation of the Troposphere, in: Issues in Atmospheric and Oceanic Modeling, edited by Saltzman, B., vol. 28 of *Advances in Geophysics*, pp. 3 – 31, Elsevier, 1985.

Held, I. M. and Suarez, M. J.: A Proposal for the Intercomparison of the Dynamical Cores of Atmospheric General Circulation Models, Bull. Amer. Meteor. Soc., 75, 1825–1830, 1994.

Hitchcock, P.: On the value of reanalyses prior to 1979 for dynamical studies of stratosphere–troposphere coupling, Atmospheric Chemistry and Physics, 19, 2749–2764, https://doi.org/10.5194/acp-19-2749-2019, 2019.

Hitchcock, P. and Haynes, P. H.: Stratospheric control of planetary waves, Geophysical Research Letters, 43, 11,884–11,892, https://doi.org/10.1002/2016GL071372, 2016.

Hitchcock, P. and Simpson, I. R.: The Downward Influence of Stratospheric Sudden Warmings, Journal of the Atmospheric Sciences, 71, 3856–3876, https://doi.org/10.1175/JAS-D-14-0012.1, 2014.

Holton, J. R. and Mass, C.: Stratospheric Vacillation Cycles, Journal of the Atmospheric Sciences, 33, 2218–2225, https://doi.org/10.1175/1520-0469(1976)033<2218:SVC>2.0.CO;2, 1976.

Hoskins, B. J.: Dynamical processes in the atmosphere and the use of models, Quarterly Journal of the Royal Meteorological Society, 109, 1–21, https://doi.org/10.1002/qj.49710945902, 1983.

Hoskins, B. J., James, I. N., and White, G.: The Shape, Propagation and Mean-Flow Interaction of Large-Scale Weather Systems, J. Atmos. Sci., 40, 1595–1612, 1983.

https://doi.org/10.5194/wcd-2020-23
Preprint. Discussion started: 26 May 2020

Jucker, M. and Reichler, T.: Dynamical Precursors for Statistical Prediction of Stratospheric Sudden Warming Events, Geophysical Research Letters, 45, 13,124–13,132, https://doi.org/10.1029/2018GL080691, 2018.

Kobayashi, S., Ota, Y., Harada, Y., Ebita, A., Moriya, M., Onoda, H., Onogi, K., Kamahori, H., Kobayashi, C., Endo, H., Miyaoka, K., and Takahashi, K.: The JRA-55 Reanalysis: General Specifications and Basic Characteristics, Journal of the Meteorological Society of Japan. Ser. II, 93, 5–48, https://doi.org/10.2151/jmsj.2015-001, 2015.

Limpasuvan, V., Thompson, D. W. J., and Hartmann, D. L.: The Life Cycle of the Northern Hemisphere Sudden Stratospheric Warmings, Journal of Climate, 17, 2584–2596, https://doi.org/10.1175/1520-0442(2004)017<2584:TLCOTN>2.0.CO;2, 2004.

Lindgren, E. A. and Sheshadri, A.: The role of wave–wave interactions in sudden stratospheric warming formation, Weather and Climate Dynamics, 1, 93–109, https://doi.org/10.5194/wcd-1-93-2020, 2020.

Lindgren, E. A., Sheshadri, A., and Plumb, R. A.: Sudden Stratospheric Warming Formation in an Idealized General Circulation Model Using Three Types of Tropospheric Forcing, Journal of Geophysical Research: Atmospheres, 123, 10,125–10,139, https://doi.org/10.1029/2018JD028537, 2018.

Martineau, P., Wright, J. S., Zhu, N., and Fujiwara, M.: Zonal-mean data set of global atmospheric reanalyses on pressure levels, Earth System Science Data, 10, 1925–1941, https://doi.org/10.5194/essd-10-1925-2018, https://www.earth-syst-sci-data.net/10/1925/2018/, 2018.

Matsuno, T.: Vertical Propagation of Stationary Planetary Waves in the Winter Northern Hemisphere, Journal of the Atmospheric Sciences, 27, 871–883, https://doi.org/10.1175/1520-0469(1970)027<0871:VPOSPW>2.0.CO;2, 1970.

Matsuno, T.: A Dynamical Model of the Stratospheric Sudden Warming, Journal of the Atmospheric Sciences, 28, 1479–1494, https://doi.org/10.1175/1520-0469(1971)028<1479:ADMOTS>2.0.CO;2, 1971.

Matthewman, N. J. and Esler, J. G.: Stratospheric Sudden Warmings as Self-Tuning Resonances. Part I: Vortex Splitting Events, Journal of the Atmospheric Sciences, 68, 2481–2504, https://doi.org/10.1175/JAS-D-11-07.1, 2011.

Pegion, K., Kirtman, B. P., Becker, E., Collins, D. C., LaJoie, E., Burgman, R., Bell, R., DelSole, T., Min, D., Zhu, Y., Li, W., Sinsky, E., Guan, H., Gottschalck, J., Metzger, E. J., Barton, N. P., Achuthavarier, D., Marshak, J., Koster, R. D., Lin, H., Gagnon, N., Bell, M., Tippett, M. K., Robertson, A. W., Sun, S., Benjamin, S. G., Green, B. W., Bleck, R., and Kim, H.: The Subseasonal Experiment (SubX): A Multimodel Subseasonal Prediction Experiment, Bulletin of the American Meteorological Society, 100, 2043–2060, https://doi.org/10.1175/BAMS-D-18-0270.1, 2019.

Phillips, N. A.: Geostrophic motion, Rev. Geophys., 1, 123–175, 1963.

Plumb, R. A.: Instability of the Distorted Polar Night Vortex: A Theory of Stratospheric Warmings, Journal of the Atmospheric Sciences, 38, 2514–2531, https://doi.org/10.1175/1520-0469(1981)038<2514:IOTDPN>2.0.CO;2, 1981.

Poli, P., Hersbach, H., Dee, D. P., Berrisford, P., Simmons, A. J., Vitart, F., Laloyaux, P., Tan, D. G. H., Peubey, C., Thépaut, J.-N., Trémolet, Y., Hólm, E. V., Bonavita, M., Isaksen, L., and Fisher, M.: ERA-20C: An Atmospheric Reanalysis of the Twentieth Century, Journal of Climate, 29, 4083–4097, https://doi.org/10.1175/JCLI-D-15-0556.1, 2016.

Polvani, L. M. and Kushner, P. J.: Tropospheric response to stratospheric perturbations in a relatively simple general circulation model, Geophys. Res. Lett., 29, 18–1–18–4, 2002.

Schoeberl, M. R.: Stratospheric warmings: Observations and theory, Reviews of Geophysics, 16, 521–538, https://doi.org/10.1029/RG016i004p00521, 1978.

Scinocca, J. F. and Haynes, P. H.: Dynamical Forcing of Stratospheric Planetary Waves by Tropospheric Baroclinic Eddies, Journal of the Atmospheric Sciences, 55, 2361–2392, https://doi.org/10.1175/1520-0469(1998)055<2361:DFOSPW>2.0.CO;2, 1998.

https://doi.org/10.5194/wcd-2020-23
Preprint. Discussion started: 26 May 2020

Scott, R. K. and Polvani, L. M.: Stratospheric control of upward wave flux near the tropopause, Geophysical Research Letters, 31, https://doi.org/10.1029/2003GL017965, 2004.

Scott, R. K. and Polvani, L. M.: Internal Variability of the Winter Stratosphere. Part I: Time-Independent Forcing, Journal of the Atmospheric Sciences, 63, 2758–2776, https://doi.org/10.1175/JAS3797.1, 2006.

Sheshadri, A., Plumb, R. A., and Gerber, E. P.: Seasonal variability of the polar stratospheric vortex in an idealised AGCM with varying tropospheric wave forcing, J. Atmos. Sci., 72, 2248–2266, 2015.

Sjoberg, J. P. and Birner, T.: Transient Tropospheric Forcing of Sudden Stratospheric Warmings, Journal of the Atmospheric Sciences, 69, 3420–3432, https://doi.org/10.1175/JAS-D-11-0195.1, 2012.

Sjoberg, J. P. and Birner, T.: Stratospheric Wave–Mean Flow Feedbacks and Sudden Stratospheric Warmings in a Simple Model Forced by Upward Wave Activity Flux, Journal of the Atmospheric Sciences, 71, 4055–4071, https://doi.org/10.1175/JAS-D-14-0113.1, 2014.

Smagorinsky, J.: The dynamical influence of large-scale heat sources and sinks on the quasi-stationary mean motions of the atmosphere, Quart. J. Roy. Meteor. Soc., 79, 342–366, https://doi.org/10.1002/qj.49707934103, 1953.

Thompson, D. W. J., Baldwin, M. P., and Wallace, J. M.: Stratospheric Connection to Northern Hemisphere Wintertime Weather: Implications for Prediction, Journal of Climate, 15, 1421–1428, https://doi.org/10.1175/1520-0442(2002)015<1421:SCTNHW>2.0.CO;2, 2002.

Tripathi, O. P., Charlton-Perez, A., Sigmond, M., and Vitart, F.: Enhanced long-range forecast skill in boreal winter following stratospheric strong vortex conditions, Environmental Research Letters, 10, 104 007, https://doi.org/10.1088/1748-9326/10/10/104007, 2015.

Vallis, G. K.: Atmospheric and Oceanic Fluid Dynamics, Cambridge University Press, 2006.

Vitart, F., Ardilouze, C., Bonet, A., Brookshaw, A., Chen, M., Codorean, C., Déqué, M., Ferranti, L., Fucile, E., Fuentes, M., Hendon, H., Hodgson, J., Kang, H.-S., Kumar, A., Lin, H., Liu, G., Liu, X., Malguzzi, P., Mallas, I., Manoussakis, M., Mastrangelo, D., MacLachlan, C., McLean, P., Minami, A., Mladek, R., Nakazawa, T., Najm, S., Nie, Y., Rixen, M., Robertson, A. W., Ruti, P., Sun, C., Takaya, Y., Tolstykh, M., Venuti, F., Waliser, D., Woolnough, S., Wu, T., Won, D.-J., Xiao, H., Zaripov, R., and Zhang, L.: The Subseasonal to Seasonal (S2S) Prediction Project Database, Bulletin of the American Meteorological Society, 98, 163–173, https://doi.org/10.1175/BAMS-D-16-0017.1, 2017.

White, I., Garfinkel, C. I., Gerber, E. P., Jucker, M., Aquila, V., and Oman, L. D.: The Downward Influence of Sudden Stratospheric Warmings: Association with Tropospheric Precursors, Journal of Climate, 32, 85–108, https://doi.org/10.1175/JCLI-D-18-0053.1, 2019.

https://doi.org/10.5194/wcd-2020-23
Preprint. Discussion started: 26 May 2020

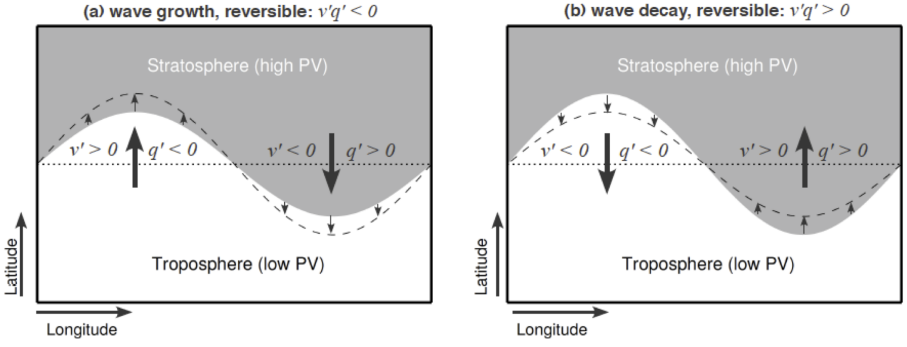

Figure 1. A schematic of a reversible wave growth (a) and decay (b) at the tropopause in a horizontal plane. Grey shading represents high PV air (from the stratosphere; PV also generally increases towards the pole), no shading (white) represents low PV air (from the troposphere; PV also generally decreases towards the Equator). Arrows denote the movements of the air as the wave grows or decays; v' represents meridional movements; q' represents changes in the PV following the meridional movements. Recall that $[v'q']$ is EP flux divergence (only for the QG dynamics). For a detailed description of the schematic see text.

https://doi.org/10.5194/wcd-2020-23
Preprint. Discussion started: 26 May 2020

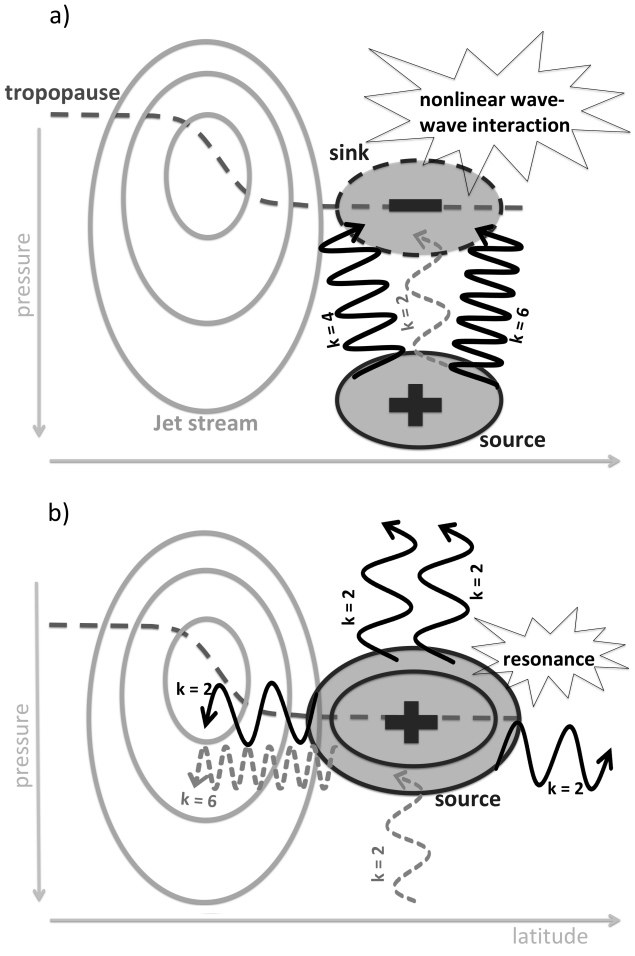

Figure 2. A schematic of upscale cascade at the tropopause in a vertical cross section: (a) smaller scale waves (e.g. $k = 4, 6$) show a sink of wave activity (i.e., EP flux convergence) at the tropopause, resulting in nonlinear wave-wave interactions; (b) an enhanced wave source appears in larger scale waves (e.g. $k = 2$), caused by upscale cascade and resonance. For detailed description of the processes see text. Grey solid contours represent zonal mean zonal wind marking the jet stream; black solid (with plus sign in the middle) and dashed (with minus sign in the middle) ellipses represent wave sources ($\nabla \cdot \mathbf{F} > 0$) and sinks ($\nabla \cdot \mathbf{F} < 0$), respectively (the number of contours signifies the strength of $\nabla \cdot \mathbf{F}$); thick dark grey dashed line represents tropopause; solid black wiggly arrows (number of wiggles corresponding to the wave's wavenumber k, as labeled) represent the waves (and their propagation direction) that have the most importance at that stage in the process; grey dashed wiggly lines correspond to waves that may be present at that stage of the process but are not necessary. Note that $k = 2$ upward propagating wave represented by grey dashed line in both panels signifies a presence of a $k = 2$ wave that can interact with the waves generated via upscale cascade, leading to a resonant behaviour.

https://doi.org/10.5194/wcd-2020-23
Preprint. Discussion started: 26 May 2020

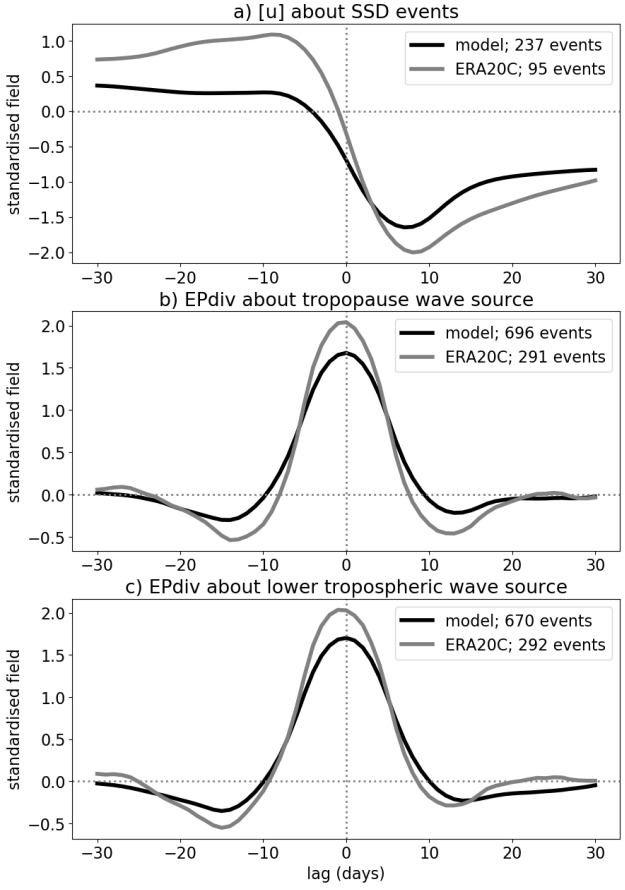

Figure 3. Index definitions shown through lag-composites of the relevant standardised quantities: (a) zonal mean zonal wind about SSD events, (b) EP flux divergence ($k = 2$ for the model, $k = 1$ for ERA-20C) at tropopause about the tropopause wave source events, and (c) EP flux divergence ($k = 2$ for the model, $k = 1$ for ERA-20C) in the lower troposphere about the surface wave source events. Lag zero is the date when the index maximises (i.e. index central date). The lines denote different datasets: black lines for the model and grey lines for ERA-20C. Note that the data was smoothed by 10-day running mean before plotting.

https://doi.org/10.5194/wcd-2020-23
Preprint. Discussion started: 26 May 2020

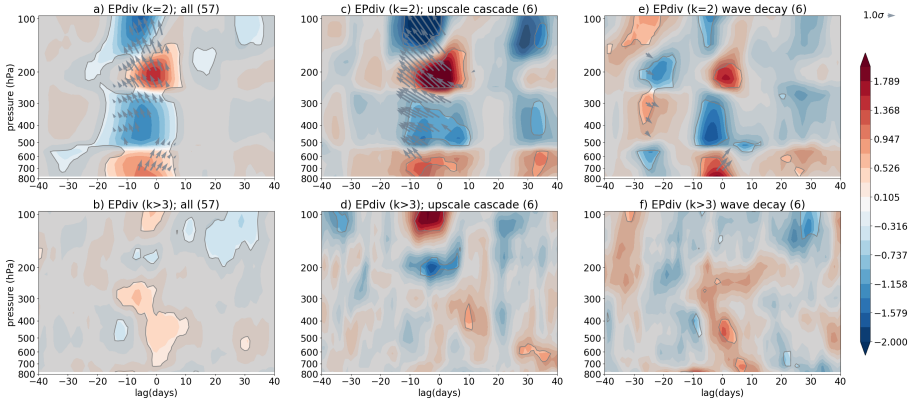

Figure 4. Composite analysis (lag-pressure for data averaged between 40 and 60°N) demonstrating the upscale cascade mechanism (based on a few subjectively identified events) (c,d) and wave decay (e,f) mechanisms, as well as a composite over all wave source events (a,b) preceding SSDs that were objectively identified. Top row (a,c,e) shows standardised $k = 2$ EP flux divergence anomalies (shading) and standardised EP flux anomalies (grey arrows), whereas bottom row (b,d,f) shows standardised EP flux divergence anomalies of the synoptic scale waves ($k \geq 4$). The arrows denote average wave propagation direction (left-tilt: equatorward; right-tilt: poleward) and its magnification within the chosen latitudinal range at specified pressure/lag, but do not imply actual size of the EP fluxes or the propagation out of the boundaries of the latitudinal range. Grey shading masks out data that are not significant at 95% level. EP fluxes (arrows) are only shown for values exceeding 95% significance level. The numbers in brackets denote the number of events in each composite. Data are from the model.

https://doi.org/10.5194/wcd-2020-23
Preprint. Discussion started: 26 May 2020

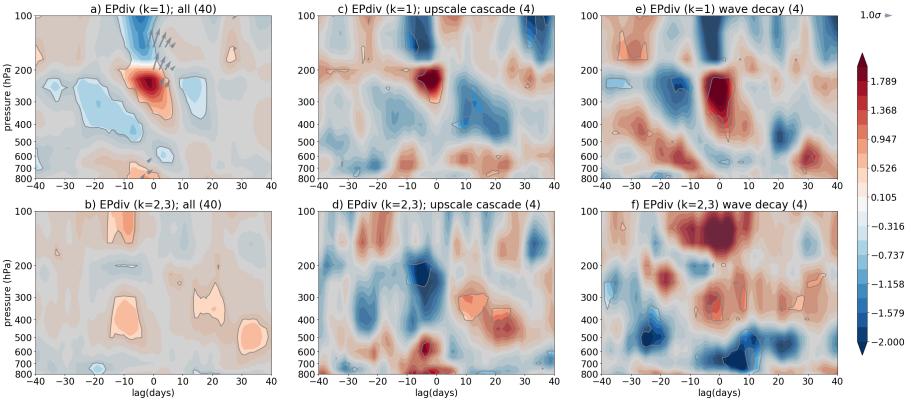

Figure 5. Similar to Fig. 4 but for ERA-20C data. Note that here top row represents the same quantities for $k = 1$ waves and bottom row represents the same quantities for $k = 2, 3$ waves instead of synoptic waves. Data are averaged between 45 and 75°N.

https://doi.org/10.5194/wcd-2020-23
Preprint. Discussion started: 26 May 2020

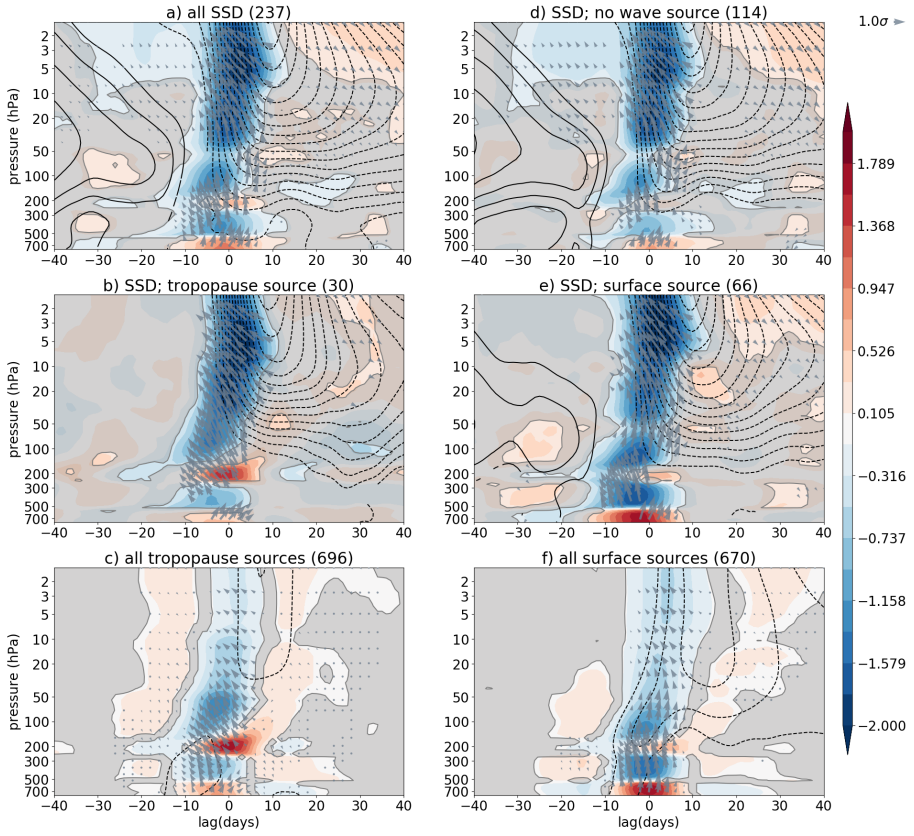

Figure 6. Composite analysis (lag-pressure for data averaged between 40 and 60°N) showing $k = 2$ standardised EP flux divergence anomalies (shading), $k = 2$ standardised EP flux anomalies (arrows), and standardised zonal mean zonal wind anomalies (contours; contour interval is 0.1, i.e. ...,-0.15, -0.05, 0.05, 0.15,...). The composites are shown for (a) all SSD events, (b) SSD events preceded by $k = 2$ tropopause wave source, (c) all $k = 2$ tropopause wave source events, (d) SSD events not preceded by $k = 2$ wave source events, (e) SSD events preceded by $k = 2$ lower-tropospheric wave source events, and (f) all $k = 2$ lower-tropospheric wave source events. (a,b,d,e) are centred around SSD events, whereas (c,f) are centred around wave source events. Grey shading masks out data that are not significant at 95% level. EP fluxes (arrows) and zonal mean zonal wind anomalies (contours) are only shown for values exceeding 95% significance level. As in Fig. 4, the arrows denote average wave propagation direction (left-tilt: equatorward; right-tilt: poleward) and its magnification within the chosen latitudinal range at specified pressure/lag. Numbers in brackets denote number of events in each composite. Data are from the model.

https://doi.org/10.5194/wcd-2020-23
Preprint. Discussion started: 26 May 2020

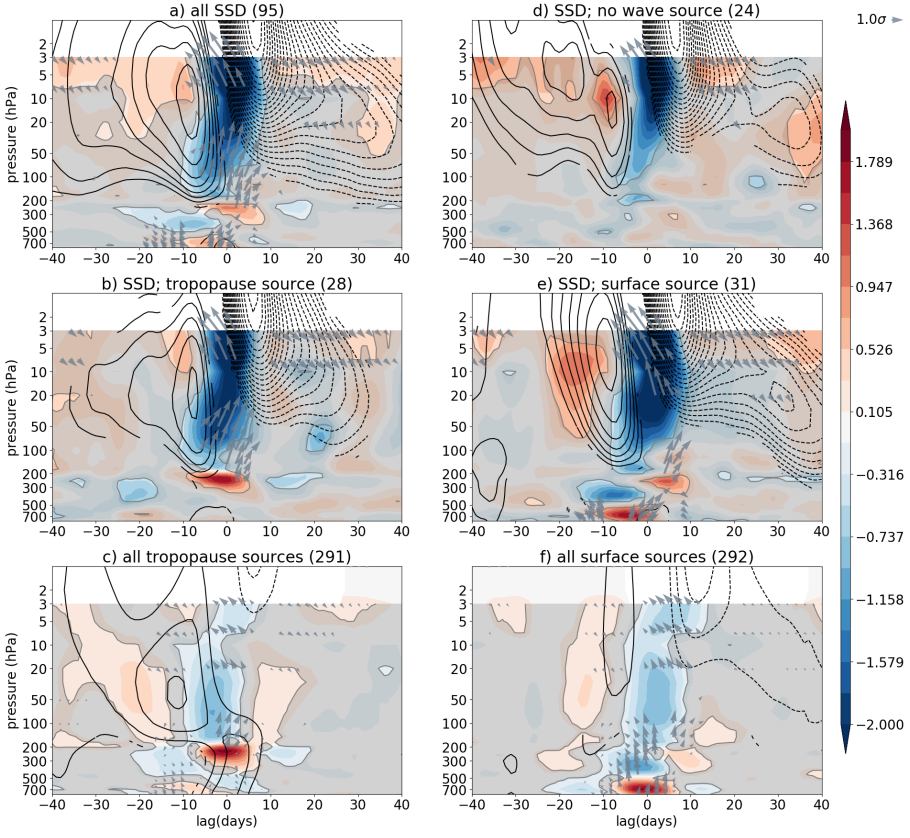

Figure 7. Similar to Fig. 6 but for ERA-20C data. Note that here the $k = 1$ standardised EP flux divergence and standardised EP fluxes (shading and arrows, respectively) are shown (and $k = 1$ wave source events were identified). Data are averaged between 45 and 75°N.

https://doi.org/10.5194/wcd-2020-23
Preprint. Discussion started: 26 May 2020

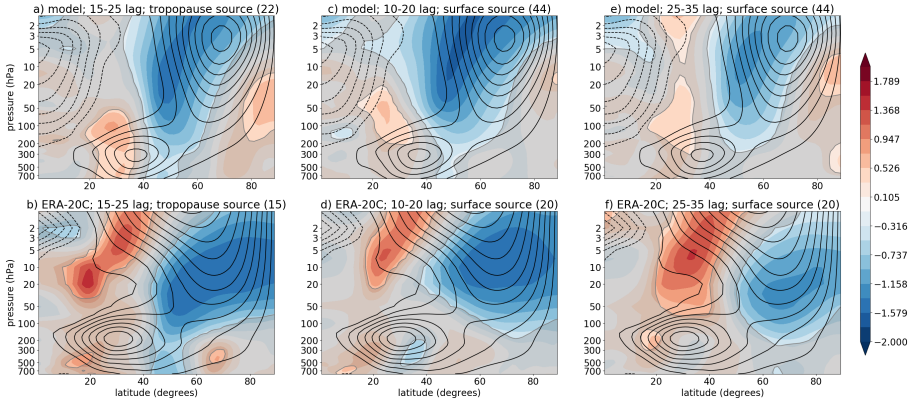

Figure 8. Composite analysis of downward impact in zonal mean zonal wind (latitude-pressure vertical cross section) averaged between the lags 15 and 25 days following an SSW event preceded by tropopause wave source event (a,b), averaged between the lags 10 and 20 days following an SSW event preceded by surface wave source event (c,d), and averaged between the lags 25 and 35 days following an SSW event preceded by surface wave source event (e,f). The figure shows standardised zonal mean zonal wind anomalies (shading) and zonal mean zonal wind climatology (contours; contour interval is 5 m s^{-1} with 0^{th} contour omitted for clarity, i.e. ...,-10, -5, 5, 10,...) for (a,c,e) model, and (b,d,f) ERA-20C. Grey shading masks out data that are not significant at 95% level. Numbers in brackets denote number of events in each composite.

https://doi.org/10.5194/wcd-2020-23
Preprint. Discussion started: 26 May 2020

Weather and Climate Dynamics Discussions
Open Access
EGU

Table 1. Total number of events (and percentage of all events) related to planetary wave sources and SSDs (as labeled). The numbers of events are also listed in Figs. 3, 6, 7.

events / all events	model	ERA-20C
SSDs with tropopause wave source / all tropopause wave source	30 / 696 (4.3%)	28 / 291 (9.6%)
SSDs with surface wave source / all surface wave source	66 / 670 (9.9%)	31 / 292 (10.6%)
SSDs with tropopause wave source / all SSDs	30 / 237 (12.7%)	28 / 95 (29.5%)
SSDs with surface wave source / all SSDs	66 / 237 (27.8%)	31 / 95 (32.6%)
SSDs without wave sources / all SSDs	114 / 237 (48.1%)	24 / 95 (25.3%)
SSDs with both wave sources / all SSDs	27 / 237 (11.4%)	10 / 95 (10.5%)